Valence Shell Electron Pair Interactions in H_2O and H_2S. A Test of the Valence Shell Electron Pair Repulsion Theory

William E. Palke* and Bernard Kirtman

Contribution from the Department of Chemistry, University of California, Santa Barbara, California 93106. Received December 14, 1977

Abstract: The repulsions between valence shell electron pairs are determined as a function of bond angle for H_2O and H_2S. Localized Hartree–Fock and relaxed orthogonal Hartree product calculations are used to calculate Coulomb, exchange, and overlap (Pauli principle) repulsions. Some agreement with the assumptions of VSEPR theory are found, but the bond–bond repulsions affect the equilibrium geometry more strongly than do lone pair–lone pair or bond–lone pair repulsions. We conclude that a simple physical explanation of the equilibrium bond angles in H_2O and H_2S remains to be given.

I. Introduction

The valence shell electron pair repulsion (VSEPR) theory[1] has become the standard explanation of equilibrium values of bond angles at introductory and advanced levels of chemistry. This theory is based on the assumption that molecular geometries are determined by the repulsions of pairs of electrons with lone pair–lone pair (ll′) repulsions being larger than bond–lone pair (bl) repulsions and the latter being larger than bond–bond (bb′) repulsions. The few simple rules of the method predict the correct geometry semiquantitatively for innumerable molecules both simple and complex. The origin of the pair repulsions is presumed to arise from two sources: (1) the Coulomb repulsion between pairs of electrons, and (2) the repulsion that originates from the Pauli principle which, for a molecular orbital wave function, prohibits two electrons of the same spin from occupying the same orbital. There has been disagreement as to the relative importance of these two terms, but both exist. We have determined a measure of the effect of each on the bond angle in H_2O and H_2S. Another contribution to the bending potential, that also results from the Pauli principle, is the exchange energy, which we have evaluated as well.

The Hartree–Fock (HF) method predicts fairly accurate equilibrium bond angles and bending force constants, so it must describe those interactions that determine molecular geometries. Therefore, we have used HF calculations as a basis from which to study individual localized orbital interactions. Coulomb and exchange integrals as well as total valence Coulomb and exchange energies were determined. For H_2O, these quantities have been reported previously, but the comparison with H_2S which reveals significant differences has not been made. In addition, the repulsion due to the orthogonality requirements imposed on the orbitals by the Pauli principle was examined. This was done by relaxing the orthogonality constraints, letting the orbitals mix, and observing the extent of mixing as well as the energy change. Previous studies have employed similar methods to show that the orbital orthogonality constraints produce the principal contribution to internal rotation barriers in several molecules.[3,4] However, the exchange energy also turns out to be an important component in some rotation barriers.[4]

II. Calculations

Calculations were carried out at several bond angles for each molecule with the OH or SH bond distance fixed at the experimental value.[5] The bases consisted of a double ζ set of Slater functions plus a set of d orbitals on the central atom.[6,7] These sets yield reasonable HF potential curves, and the one electron properties calculated for H_2O are in good agreement

with experiment.[7] So the bases are sufficiently accurate for this study.

A. H_2O. HF energies (all energies given in this paper are in hartrees; one hartree = 627.5 kcal/mol) for H_2O at angles from 60 to 180° are listed in Table I. The effect of exchange energy on the potential curve was examined using two different methods. In one the HF orbitals were localized by an Edmiston–Ruedenberg transformation,[8] and the resulting localized exchange energy was subtracted from the total to give the values shown in Table I. A second measure of the exchange energy contribution was obtained from an orthogonal Hartree product (OHP) calculation.[4] A Hartree product wave function is a nonsymmetrized product of doubly occupied orbitals. If these orbitals are constrained to be orthogonal, a variation principle exists for the energy. So the OHP wave function is the best doubly occupied orbital wave function without exchange. The HF wave function, on the other hand, is the best doubly occupied orbital wave function with exchange. Thus, the energy difference between the two calculations represents an exchange contribution. This contribution usually agrees closely with the localized HF (LHF) result. This is not surprising because the LHF wave function equals the antisymmetrized OHP wave function that is restricted to the space of the occupied HF orbitals, and that space is a good one for describing the energy and properties of a molecule. Our values for the OHP energy are included in Table I. The potential curves predicted by the HF energy minus localized exchange and by the OHP calculations are very similar. They each predict a slight shift in the minimum of about 2° toward smaller angles and a somewhat steeper bending potential than does HF. The HF and the HF minus localized exchange energies are plotted relative to one another in Figure 1. It is interesting that the exchange energy itself has a maximum near the equilibrium angle.

The individual Coulomb and exchange integrals are measures of the repulsive interactions between electron pairs. Values for these integrals over the LHF orbitals are shown in Table I and the Coulomb integrals are plotted in Figure 2. (The plot of OHP Coulomb integrals differs negligibly from this.) As supposed in VSEPR theory, and found by Naleway and Schwartz, the lone pair–lone pair Coulomb integrals ($J_{ll'}$) are largest followed by lone pair–bond (J_{bl}) and then by bond–bond ($J_{bb'}$) Coulomb repulsions. However, it is the slope of the curves that gives the effect of each term on the bond angle, and $J_{bb'}$ has the largest slope. Since the latter favors a larger angle the minimum in a plot of $J_{bb'}$ plus $J_{ll'}$ vs. angle occurs between 115 and 120°. Although J_{bl} varies only slightly with angle, its total effect is four times the number given because there are four bond–lone pair interactions in H_2O. This is sufficient to shift the minimum in the total valence shell electron pair

Table I. Total Energies and Coulomb and Exchange Integrals for H_2O

| angle, deg	total energies			Coulomb integrals				exchange integrals			
	HF	HF-loc exch	OHP	$J_{bb'}$	$J_{ll'}$	J_{bl}	ΣJ valence	$K_{bb'}$	$K_{ll'}$	K_{bl}	ΣK valence
60	−75.9630	−75.2332	−75.3058	0.6004	0.6479	0.6171	14.8660	0.0477	0.0487	0.0497	0.5900
90	−76.0277	−75.3319	−75.3964	0.5767	0.6617	0.6140	14.7776	0.0367	0.0556	0.0463	0.5548
95	−76.0312	−75.3366	−75.4007	0.5736	0.6635	0.6140	14.7728	0.0360	0.0564	0.0461	0.5532
100	−76.0330	−75.3385	−75.4026	0.5706	0.6653	0.6142	14.7712	0.0355	0.0572	0.0459	0.5528
104.5	−76.0333	−75.3383	−75.4024	0.5684	0.6668	0.6145	14.7720	0.0352	0.0578	0.0459	0.5528
109.5	−76.0322	−75.3357	−75.4000	0.5661	0.6684	0.6149	14.7760	0.0351	0.0585	0.0459	0.5540
115	−76.0294	−75.3302	−75.3951	0.5640	0.6702	0.6155	14.7844	0.0351	0.0592	0.0459	0.5564
120	−76.0257	−75.3230	−75.3887	0.5625	0.6718	0.6161	14.7952	0.0354	0.0598	0.0461	0.5592
150	−75.9898	−75.2424	−75.3183	0.5640	0.6794	0.6229	14.9400	0.0418	0.0616	0.0492	0.6008
180	−75.9672	−75.1317	−75.2115								
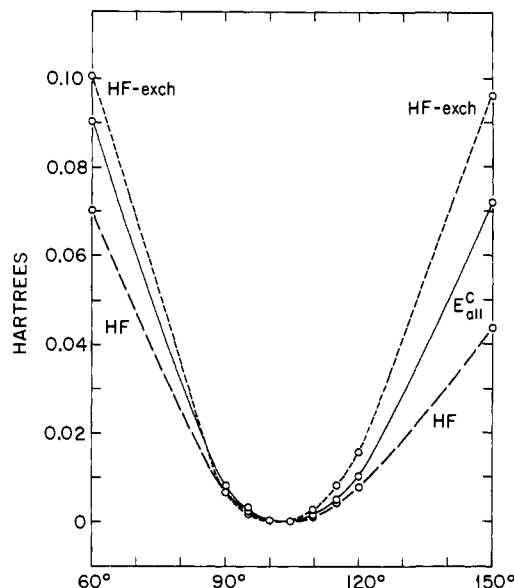
Figure 1. Variation with bond angle of the HF energy (HF), the HF energy minus localized exchange (HF − exch), and the constraint energy for relaxing all valence orthogonalities (E_{all}^c) in H_2O. Each energy is plotted relative to its value at equilibrium.
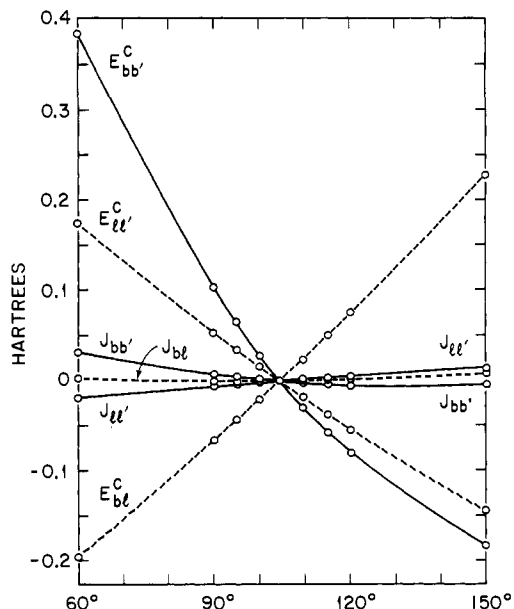

Figure 2. Variation with bond angle of the individual pair Coulomb integrals (J) and constraint energies (E^c) for H_2O. Subscripts b and l refer to bond and lone pairs, respectively. Each quantity is plotted relative to its value at equilibrium.

Coulomb repulsion, also listed in Table I, to the equilibrium angle. Furthermore, this Coulomb repulsion energy shows nearly the same angle dependence as the complete HF potential curve.

The exchange integrals are more than an order of magnitude smaller than the Coulomb integrals. They show roughly the same behavior vs. angle as the Coulomb integrals, and their effect on the total interaction $2J − K$, although small, is not negligible. The exchange energy lowers the sides of the curve relative to the minimum making it less steep. This effect can be seen in Figure 1.

Because the antisymmetrizer effectively orthogonalizes doubly occupied orbitals in a wave function, an orbital product cannot be antisymmetrized completely if the orbital orthogonality constraint is to be relaxed. To study the effect of orbital orthogonality, two types of relaxation calculations were carried out for H_2O. The first approach was to begin with an orthogonal Hartree product and then simply to remove one or more of the orthogonality constraints. In each case the two bond orbitals were required to be equivalent to one another, and the lone pairs were likewise constrained. Four calculations were performed at each angle using LHF orbitals with the inner shell frozen to avoid collapse into the core. One at a time, the bb', ll', and bl pair orthogonalities were relaxed by allowing the orbitals to mix together to lower the energy of the Hartree product. Finally, all the valence shell orthogonality constraints

were removed simultaneously. The values of the overlaps between the resulting orbitals and the constraint energies are given in Table II. The latter are also plotted in Figure 2. The constraint energy is the energy decrease due to removal of the orthogonality constraint. This is a measure of the strength of the electron pair repulsion caused by the Pauli principle. Again, as presumed in VSEPR theory, the ll' constraint energy is larger than that for the bl pair and the bb' interactions. (Note that the bl pair numbers given are for the relaxation of all four orthogonality constraints.) However, just as for the Coulomb integrals, the slope of the bb' constraint energy curve is steepest, and so it has a larger effect on the equilibrium angle than ll' repulsion. Both bb' and ll' overlap repulsions favor an increased angle, whereas the bl interaction favors smaller angles. It can be seen from Table II that considerable mixing occurs in every case that an orthogonality constraint is removed. (The largest possible bl overlap is 0.5 if the bond orbitals are kept orthogonal and equivalent and the lone pairs are similarly restricted.) The relaxed wave functions violate the Pauli principle by a considerable amount, and the effect on the energy is moderately large. Removal of all the valence pair orthogonality constraints resulted in a nearly complete collapse of all eight electrons into the oxygen 2s orbital (all overlaps were 1.0000) along with a huge drop in energy. This is such a drastic violation of the Pauli principle that we are reluctant to attach too much meaning to the fact that the constraint energy

Table II. Relaxation of Orthogonality Constraints for H_2O^c

angle, deg	bb' relaxation		ll' relaxation		bl relaxation		all valence
	overlap	constraint energy	overlap	constraint energy	overlap	constraint energy[a]	constraint energy[b]
60	1.0000	0.7566	1.0000	0.6974	0.4978	1.3114 (1.2507, 1.1803)	4.2963 (2.7644)
90	1.0000	0.4742	1.0000	0.5771	0.4973	1.4483 (1.3811, 1.3251)	4.2137 (2.4996)
95	0.9704	0.4351	1.0000	0.5584	0.4973	1.4710 (1.4021, 1.3478)	4.2088 (2.4645)
100	0.9289	0.3997	0.9850	0.5399	0.4974	1.4938 (1.4231, 1.3703)	4.2062 (2.4334)
104.5	0.8936	0.3712	0.9686	0.5236	0.4975	1.5145 (1.4419, 1.3904)	4.2056 (2.4093)
109.5	0.8558	0.3420	0.9504	0.5055	0.4976	1.5381 (1.4632, 1.4132)	4.2068 (2.3856)
115	0.8164	0.3131	0.9308	0.4858	0.4978	1.5647 (1.4868, 1.4384)	4.2103 (2.3636)
120	0.7828	0.2897	0.9133	0.4683	0.4979	1.5892 (1.5083, 1.4614)	4.2155 (2.3472)
150	0.6129	0.1889	0.8287	0.3779	0.4992	1.7417 (1.6379, 1.5988)	4.2774 (2.3085)

[a] The values in parentheses are the bl relaxation constraint energies obtained with the partially antisymmetric wave function Ψ_A. The first value was obtained using the complete basis; the second was obtained using the HF orbital basis. [b] The sum of the individual pair constraint energies is given in parentheses. [c] In each case, the indicated constraint was relaxed by mixing the initial LHF orbitals so as to minimize the energy with the restriction that the two bonding (and lone pair) orbitals remain equivalent. The constraint energy is the magnitude of this energy lowering.

Table III. Total Energies and Coulomb and Exchange Integrals for H_2S

angle, deg	total energies		Coulomb integrals				exchange integrals			
	HF	HF-loc exch	$J_{bb'}$	$J_{ll'}$	J_{bl}	ΣJ valence	$K_{bb'}$	$K_{ll'}$	K_{bl}	ΣK valence
75	-398.6894	-395.4086	0.3819	0.4037	0.3811	9.2412	0.0180	0.0338	0.0374	0.4030
82	-398.6968	-395.4203	0.3739	0.4050	0.3809	9.2096	0.0164	0.0348	0.0367	0.3964
90	-398.7008	-395.4267	0.3653	0.4064	0.3809	9.1816	0.0151	0.0360	0.0360	0.3898
92.2	-398.7012	-395.4274	0.3630	0.4068	0.3810	9.1752	0.0148	0.0363	0.0357	0.3880
100	-398.6998	-395.4260	0.3555	0.4080	0.3814	9.1572	0.0140	0.0373	0.0349	0.3822
109.5	-398.6930	-395.4174	0.3475	0.4094	0.3822	9.1436	0.0134	0.0386	0.0339	0.3752

does have a minimum at the equilibrium angle giving a well that is almost twice as steep as the HF potential curve (see Figure 2). It should be noted that the constraint energies are not additive. Not only is the sum of separate pair energies considerably less than that obtained for relaxing all valence orthogonality, but that sum does not show a minimum.

The second type of orthogonality relaxation that we carried out was done using partially antisymmetric wave functions. This keeps the wave function as close to the familiar HF form as possible and serves as a check on the results discussed above. To relax the bond–lone pair orthogonality, a wave function of the form

$$\Psi_A = A(1s^2) A(b_1{}^2 b_2{}^2) A(l_1{}^2 l_2{}^2) \qquad (1)$$

was chosen. Each antisymmetrizer A operates only on the coordinates of those electrons in the orbitals in parentheses immediately following it. The 1s orbital was frozen as the LHF 1s orbital, and the bond orbitals b_1, b_2 as well as the lone pair orbitals l_1, l_2 were allowed to vary in the entire basis with the constraint that they remain orthogonal to the core. The result of the orthogonality relaxation was that the a_1 symmetry bonding orbital and the a_1 lone pair collapsed together into a nearly pure 2s orbital. The overlap of the two final orbitals was greater than 0.99 at all angles. This result is unchanged if the canonical HF orbital is used as the core. Similar calculations were carried out with the orbitals restricted to the HF space. This restriction in the basis set caused very little difference in the energy vs. angle variation. A measure of the effect of constraining the bond orbitals to be orthogonal to the lone pairs is the difference between the energy of Ψ_A calculated with LHF orbitals and with orthogonality-relaxed orbitals. This constraint energy is listed in Table II. Since there are four bond–lone pair overlaps, the constraint per interaction is one-fourth of the tabulated number. The angle variation closely parallels that of the Hartree product treatment.

In order to relax the bond–bond orthogonality constraint a wave function of the form

$$\Psi_B = A(1s^2 l_1{}^2 l_2{}^2) A(b_1{}^2) A(b_2{}^2) \qquad (2)$$

was chosen. The 1s and lone pair orbitals were frozen as the LHF functions and the LHF bond orbitals were allowed to mix together (i.e., they were restricted to the HF space). The overlaps for the two resulting bond orbitals are nearly the same as those found for the Hartree product bb' relaxation. Our constraint energies, calculated as the energy difference of Ψ_B with LHF orbitals and with relaxed orbitals, differ by less than 10^{-4} au from those of the Hartree product calculation.

Finally, the lone pair–lone pair orthogonality was studied with a wave function of the form

$$\Psi_C = A(1s^2 b_1{}^2 b_2{}^2) A(l_1{}^2) A(l_2{}^2) \qquad (3)$$

In this case, the inner shell and bond orbitals were frozen as LHF functions and the lone pairs were allowed to mix together. Overlaps between the relaxed lone pair orbitals turn out to be nearly the same as those of the corresponding Hartree product calculation. As in the previous case, the constraint energies calculated with Ψ_C also agree with those of the Hartree product calculations to four decimal places.

The partially antisymmetrized wave function and the Hartree product results agree very closely for the variation in relaxation quantities vs. angle. In addition, restricting the orbitals to the HF space makes little difference in the outcome.

B. H_2S. Calculations were carried out on H_2S at bond angles from 75° to tetrahedral. The HF energy by itself and with the localized exchange energy subtracted are listed in Table III. These quantities are also plotted in Figure 3. (Considerable mixing of the 2s and 2p orbitals caused the Edmiston–Ruedenberg LHF transformation procedure to converge very slowly for H_2S.) Removal of the exchange energy does not affect the position of the minimum significantly, but just as for H_2O, it makes the potential curve a bit steeper. Again, the total exchange energy is least negative near the equilibrium angle.

Table IV. Relaxation of Orthogonality Constraints for H_2S^b

| angle, deg | bb' relaxation | | ll' relaxation | | bl relaxation | | all valence |
	overlap	constraint energy	overlap	constraint energy	overlap	constraint energy	constraint energy^a
75	0.7330	0.1877	0.9367	0.3258	0.4664	0.5466	1.7718 (1.0601)
82	0.6667	0.1573	0.9080	0.3094	0.4672	0.5636	1.7526 (1.0303)
90	0.5996	0.1285	0.8757	0.2910	0.4686	0.5841	1.7380 (1.0036)
92.2	0.5828	0.1217	0.8664	0.2857	0.4690	0.5899	1.7349 (0.9973)
100	0.5292	0.1014	0.8334	0.2669	0.4708	0.6118	1.7293 (0.9801)
109.5	0.4749	0.0825	0.7914	0.2433	0.4734	0.6404	1.7299 (0.9662)

^{a} The sum of the individual pair constraint energies is given in parentheses. ^{b} In each case, the indicated constraint was relaxed, by mixing the initial LHF orbitals so as to minimize the energy with the restriction that the two bonding (and lone pair) orbitals remain equivalent. The constraint energy is the magnitude of this energy lowering.
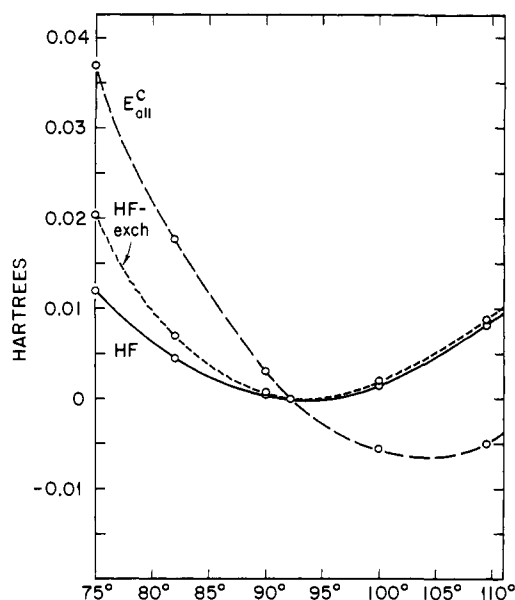
Figure 3. Variation with bond angle of the HF energy (HF), the HF energy minus localized exchange (HF − exch), and the constraint energy for relaxing all valence orthogonalities (E_{all}^c) in H_2S. Each energy is plotted relative to its value at equilibrium.
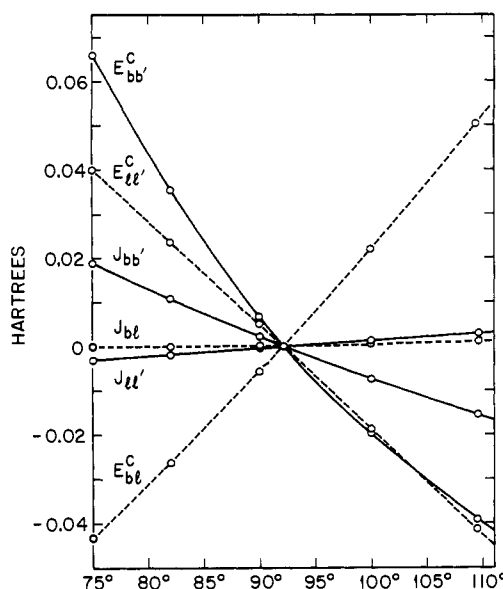
Figure 4. Variation with bond angle of the individual pair Coulomb integrals (J) and constraint energies (E^c) in H_2S. Subscripts b and l refer to bond and lone pairs, respectively. Each quantity is plotted relative to its value at equilibrium.

Coulomb integrals over the LHF orbitals are listed in Table III and plotted in Figure 4. Just as in H_2O, $J_{ll'}$ is largest followed by J_{bl} and $J_{bb'}$. Again, as we found for H_2O, $J_{bb'}$ shows the largest angle dependence. In fact, for H_2S this term dominates the sum of the valence shell Coulomb repulsions. As a result, the sum monotonically decreases over the entire angle range (from 75 to 109.5°) which is quite different from H_2O for which the corresponding Coulomb energy parallels the HF potential curve.

The LHF exchange integrals over valence orbitals are also given in Table III. Since the valence shell exchange energy does not, by itself, have a maximum at the equilibrium angle this maximum must arise from inner shell terms in contrast with H_2O.

Effects due to orthogonality constraints in H_2S were determined from Hartree product wave functions with the core (K and L shells) frozen as localized HF orbitals. The relaxed orbitals were restricted to the HF space because full basis set calculations are expensive, and our H_2O results indicate that the added basis functions would make little difference. One at a time, the bb', ll', and bl orthogonality constraints were removed as before. Overlaps between the relaxed orbitals as well as the constraint energies are given in Table IV. Although the extent of mixing is somewhat less than in H_2O, the qualitative results are the same. Mixing is substantial. The ll' orthogonality constraint energy is largest, but the bb' term has a larger slope (see Figure 4). Further calculations were carried

out with all valence orthogonality constraints removed simultaneously. Even though the drop in energy is not as large as for H_2O, the collapse is nearly complete into a 3s-like orbital. (All overlaps were 1.0000.) The constraint energies for this calculation are listed in Table IV and plotted in Figure 3. Just as for H_2O, this shows a minimum. However, the well is steeper than the HF potential curve and the minimum occurs at more than 10° greater than the equilibrium angle. The position of this minimum and the shape of the curve are very similar to the analogous H_2O results. Once again, we find that constraint energies are not pairwise additive.

III. Summary

For both H_2O and H_2S the lone pair-lone pair repulsions (Coulomb and overlap) are larger than bond-lone pair or bond-bond repulsions. This agrees with the assumptions of VSEPR theory. However, in both molecules the bond-bond repulsions exert the largest effect on the equilibrium geometry because they have the largest slope vs. bond angle.

Bond-bond repulsion forces (Coulomb and overlap) do not become small at angles a few degrees greater than bond angles predicted by VSEPR hybridization (tetrahedral for H_2O and 90° for H_2S if d orbitals participate). Both are still large in H_2O at 120° and in H_2S at 110°. The direction of the forces is the same in both molecules—bb' repulsions (Coulomb and overlap) favor larger angles, ll' Coulomb repulsion favors small angles, but ll' overlap repulsion is in the opposite direction. The

bl Coulomb integrals are nearly angle independent and bl pair overlap repulsion favors small angles.

The sum of valence shell Coulomb repulsions mimics the HF potential curve accurately for H_2O but does not even show a minimum for H_2S. Similarly, the constraint energy for relaxing all valence overlap constraints mimics the HF potential curve well for H_2O but poorly for H_2S. One must be careful of the interpretation of this because the orthogonality relaxation causes all eight valence electrons to collapse into one s-like orbital. The total exchange energy over LHF orbitals has a small (compared to the HF energy curve) maximum near the equilibrium angle for both molecules. However, in H_2S, it is the inner shell terms that create this maximum. We conclude that some of the assumptions of VSEPR theory are borne out by our calculations, but many are not. A simple explanation of the equilibrium bond angles in H_2O and H_2S in terms of the physical interactions in the molecule remains to be given.

The present results do not contradict the notion that the bonds in these molecules are formed primarily of p orbitals[9] rather than tetrahedral hybrids. Perhaps the problem is best studied from this viewpoint.[10] The situation is complicated by the presence of bent bonds that do not appreciably follow the nuclei during bending.[11]

References and Notes

(1) N. Sidgwick and H. Powell, *Proc. R. Soc. London, Ser. A*, **176**, 153 (1940); R. Gillespie and R. Nyholm, *Q. Rev., Chem. Soc.*, **11**, 339 (1957); R. Gillespie, *J. Chem. Educ.*, **47**, 18 (1970); **51**, 367 (1974).
(2) C. A. Naleway and M. E. Schwartz, *J. Am. Chem. Soc.*, **95**, 8235 (1973).
(3) O. J. Sovers, C. W. Kern, R. M. Pitzer, and M. Karplus, *J. Chem. Phys.*, **49**, 2592 (1968); C. W. Kern, R. M. Pitzer, and O. J. Sovers, *ibid.*, **60**, 3583 (1974).
(4) P. A. Christiansen and W. E. Palke, *J. Chem. Phys.*, **67**, 57 (1977). See also M. Levy, T. S. Nee, and R. G. Parr, *ibid.*, **63**, 316 (1975); P. A. Christiansen and W. E. Palke, *Chem. Phys. Lett.*, **31**, 462 (1975).
(5) For H_2O: G. Herzberg, "Infrared and Raman Spectra of Polyatomic Molecules", Van Nostrand, Princeton, N.J., 1945. More accurate results are given by W. S. Benedict, N. Gailar, and E. K. Plyler, *J. Chem. Phys.*, **24**, 1139 (1965). For H_2S: H. C. Allen and E. K. Plyler, *ibid.*, **25**, 1132 (1956).
(6) D. M. Chipman, B. Kirtman, and W. E. Palke, *J. Chem. Phys.*, **65**, 2556 (1976).
(7) D. M. Chipman, B. Kirtman, and W. E. Palke, unpublished results.
(8) C. Edmiston and K. Ruedenberg, *Rev. Mod. Phys.*, **35**, 457 (1963). At 180° the LHF orbitals are not two bonds and two lone pairs but consist of one orbital containing large coefficients from basis functions on both hydrogens plus three nearly equivalent pairs. Thus, subsequent calculations based on bond and lone pairs were not performed for this case.
(9) L. Pauling, "The Nature of the Chemical Bond", 3rd ed, Cornell University Press, Ithaca, N.Y., 1960, p 90.
(10) J. Jarvie, W. Willson, J. Doolittle, and C. Edmiston, *J. Chem. Phys.*, **59**, 3020 (1973).
(11) D. M. Chipman, W. E. Palke, and B. Kirtman, to be published.

Influence of Substituents upon Ionization Potential. Dependence of the π-Ionization Energy on the Orientation of an Allylic Hydroxyl or Methoxyl Substituent

R. S. Brown* and Randall W. Marcinko

Contribution from the Department of Chemistry, University of Alberta, Edmonton, Alberta, Canada T6G 2G2. Received March 29, 1978

Abstract: The dependence of the π-ionization energy of some allylic alcohols and ethers of rigid geometry was investigated by photoelectron spectroscopy. The π bond was found to be most stabilized (hardest to ionize) when the allylic C–O bond is coplanar with the π system, and becomes progressively less stabilized (relative to the parent olefin with no substituent) as the allylic C–O bond is perpendicular to the π bond. This observed dependence of π-IP on orientation is consistent with (a) a hyperconjugative σ*–π stabilization of the olefin when the adjacent σ* bond is coplanar; (b) a reinforcing inductive stabilization of the olefin which is independent of orientation; and (c) an opposing through-bond destabilization of the π bond when the allylic C–O bond is orthogonal to the olefin. An evaluation of some of the available literature data in the light of the present observations is presented.

I. Introduction

The mechanisms by which substituents remote from each other interact and thereby alter their respective properties merits continued experimental and theoretical investigation. Substituent effects are commonly considered in terms of inductive[1] and conjugative[2] components with the former depending largely on the differences in electronegativity of the interacting groups as well as their separation, and the latter depending upon the mutual interaction of orbitals of like symmetry. Usually the two operate simultaneously to reinforce or oppose each other, thereby introducing uncertainty into quantifying one or the other effect.

Recently our attention was drawn to a series of theoretical studies by Pople et al.[3] who have considered the interaction of two electronegative groups bridged by a methylene unit. According to the bond separation energies as defined for eq 1,[3] when both X and Y are "heavy groups" such as CH_3, NH_2, OR, or F, the calculated energy of the left is lower than that

$$Y{\diagdown}CH_2{-}\ddot{X} + H{\diagdown}CH_2{-}H$$
$$\rightleftharpoons Y{\diagdown}CH_2{-}H + H{\diagdown}CH_2{-}\ddot{X} \quad (1)$$
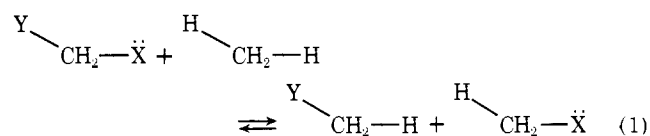
of the right side of eq 1, corresponding to a stabilization of the larger molecule. The findings were interpreted[3] as arising from a π-type donation from X and a σ (σ*) acceptance by the polarized C–Y bond as in **1** which requires a coplanarity of the

$$Y{\diagdown}C{-}\ddot{X} \longleftrightarrow Y^-{\diagdown}C{=}X^+$$
1
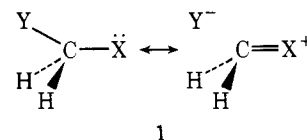
two orbitals for maximal effect. According to these calculations, there is a reduced gross population in the donor ($\ddot{X}$) orbital, and an increased π-overlap population between X and